A&A 591, L2 (2016)
DOI: 10.1051/0004-6361/201628427

Astronomy & Astrophysics

Letter to the Editor

Abundance of $HOCO^+$ and CO_2 in the outer layers of the L1544 prestellar core

C. Vastel[1,2], C. Ceccarelli[3,4], B. Lefloch[3,4], and R. Bachiller[5]

[1] Université de Toulouse, UPS-OMP, IRAP, 31013 Toulouse, France
e-mail: charlotte.vastel@irap.omp.eu
[2] CNRS, IRAP, 9 Av. Colonel Roche, BP 44346, 31028 Toulouse Cedex 4, France
[3] Université de Grenoble Alpes, IPAG, 38000 Grenoble, France
[4] CNRS, IPAG, 38000 Grenoble, France
[5] Observatorio Astronómico Nacional (OAN, IGN), Calle Alfonso XII, 3, 28014 Madrid, Spain

Received 3 March 2016 / Accepted 18 May 2016

ABSTRACT

The L1544 prestellar core has been observed as part of the ASAI IRAM Large Program at 3 mm. These observations led to the detection of many complex molecules. In this Letter, we report the detection of two lines, at 85.5 GHz ($4_{0,4}$–$3_{0,3}$) and 106.9 GHz ($5_{0,5}$–$4_{0,4}$), respectively, of the protonated carbon dioxide ion, $HOCO^+$. We also report the tentative detection of the line at 100.4 GHz ($5_{0,5}$–$4_{0,4}$) of $DOCO^+$. The non-LTE analysis of the detected lines shows that the $HOCO^+$ emission originates in the external layer where non-thermal desorption of other species has previously been observed. Its abundance is $(5 \pm 2) \times 10^{-11}$. Modelling of the chemistry involved in the formation and destruction of $HOCO^+$ provides a gaseous CO_2 abundance of 2×10^{-7} (with respect to H_2) with an upper limit of 2×10^{-6}.

Key words. astrochemistry – line: identification – molecular data – radiative transfer

1. Introduction

The protonated form of CO_2, $HOCO^+$, was first identified in the Galactic centre molecular cloud SgrB2 by Thaddeus et al. (1981). The detection was then confirmed with the laboratory detection by Bogey et al. (1984). Minh et al. (1988) reported a survey towards 18 molecular clouds (dark clouds and active star-forming regions) and concluded that the $HOCO^+$ ion was only detected towards SgrB2, and later towards SgrA (Minh et al. 1991). To date, this ion has been detected towards the Galactic centre, several translucent and dark clouds (Turner et al. 1999), a single low-mass Class 0 protostar (Sakai et al. 2008), and in the prototypical protostellar bow shock L1157-B1 (Podio et al. 2014). $HOCO^+$ was first proposed by Herbst et al. (1977) as an indirect tracer of gas-phase CO_2. Through a comparison of the abundances of $HOCO^+$ with that of HCO^+, the abundance of gas-phase CO_2 relative to that of CO might be constrained. Carbon dioxide (CO_2) is an important constituent of interstellar ices and has been widely detected in absorption towards infrared bright sources with the ISO and Spitzer telescopes. However, its formation mechanism is still not completely understood. Unfortunately, CO_2 cannot be traced in the millimeter/submillimeter regime because it lacks a permanent dipole moment, therefore it can only be sought towards sources with a bright infrared continuum. In the solid phase, its abundance represents about 15–50% of solid H_2O in quiescent molecular clouds, low-mass and high-mass protostars (Whittet et al. 1998, 2007, 2009; Öberg et al. 2011), and the ice abundances seem to be the highest for the coldest sources. The observed abundances of solid CO_2 in the interstellar medium are a factor of 100 higher than in the gas phase (van Dishoeck et al. 1996; Boonman et al. 2003a), and the formation of CO_2 is therefore assumed to proceed through reactions in the ices of interstellar dust grains. CO_2 is readily produced in UV photo-processed CO-H_2O laboratory ice, with an efficiency high enough to be driven by the cosmic-ray-induced UV field in dense interstellar regions (Watanabe & Kouchi 2002). Cosmic-ray processing of pure CO laboratory ice has also been shown to be a viable mechanism for CO_2 production in the interstellar medium (Jamieson et al. 2006) and is an interesting solution given the large abundances of pure CO ice (Pontoppidan et al. 2003). Recently, Ioppolo et al. (2011) showed a correlation between the formation of CO_2 and H_2O (under laboratory conditions), which is consistent with the astronomical observation of solid CO_2 in water-rich environments. Neill et al. (2014) performed a sensitive line survey of Sgr B2(N), and based on the $HOCO^+$ species, they estimated a CO_2/CO ratio in the colder external envelope of between 0.01–0.1, implying a CO_2 gas-phase abundance of 10^{-6}–10^{-5}, consistent with the finding of Minh et al. (1988, 1991). Their lower limit to the CO_2 gas-phase abundance of 10^{-6} relative to H_2 indicates that the CO_2 abundance in the gas is clearly enhanced, while most of the water is still frozen out in ices in the Sgr B2 envelope.

As part of the IRAM-30 m Large Program ASAI[1] (Lefloch et al., in prep.), we carried out a highly sensitive, unbiased spectral survey of the molecular emission of the L1544 prestellar core with high spectral resolution. This source is a prototypical starless core in the Taurus molecular cloud complex ($d \sim 140$ pc) on the verge of the gravitational collapse (Caselli et al. 2002, and references within). It is characterised by a central high density (2×10^6 cm^{-3}) and a low temperature (~7 K). We reported the detection of many oxygen bearing complex organic molecules produced through the release in the gas phase of methanol and

[1] Astrochemical Surveys At Iram: http://www.oan.es/asai/

Table 1. Properties of the observed $HOCO^+$ and $DOCO^+$ lines ($E_{up} \leq 30$ K).

Transitions	Frequency (MHz)	Aij (s^{-1})	E_{up} (K)	V_{peak} (km s^{-1})	$FWHM$ (km s^{-1})	$\int T_{mb} dV$ (K km s^{-1})	rms (mK)
			$HOCO^+$				
$4_{0,4}$–$3_{0,3}$	85 531.51	1.29×10^{-5}	10.26	7.25 ± 0.01	0.43 ± 0.03	0.022 ± 0.004	3.2
$5_{0,5}$–$4_{0,4}$	106 913.56	2.59×10^{-5}	15.39	7.19 ± 0.02	0.34 ± 0.04	0.013 ± 0.003	4.6
			$DOCO^+$				
$4_{0,4}$–$3_{0,3}$	80 288.79	1.14×10^{-5}	9.63			≤0.02	5.2
$5_{0,5}$–$4_{0,4}$	100 359.55	2.28×10^{-5}	14.45	6.40 ± 0.03	0.28 ± 0.06	0.004 ± 0.001	3.5
$4_{1,4}$–$3_{1,3}$	79 776.48	1.05×10^{-5}	30.07			≤0.02	4.5

Notes. The upper limits have been computed using the rms around the line. The errors in the fluxes include the calibration and statistical uncertainties from the Gaussian fits of the lines.

ethene through non-thermal desorption processes (Vastel et al. 2014, hereafter Paper I). The sensitivity of these IRAM observations also led to the detection of the hyperfine structure of CH_2CN (Vastel et al. 2015a). In the present study we report on the detection of the $HOCO^+$ ion in the L1544 prestellar core, as well as a tentative detection of its deuterated form, $DOCO^+$.

2. Observations and results

The observations were performed at the IRAM-30 m towards L1544 ($\alpha_{2000} = 05^h04^m17.21^s, \delta_{2000} = 25°10'42.8''$) using the broad-band receiver EMIR at 3 mm, connected to an FTS spectrometer in its 50 kHz resolution mode. The beam of the observations is 29″ and 23″ at 85 and 106 GHz, respectively. Line intensities are expressed in units of main-beam brightness temperature (see Paper I for more details).

The frequencies and other spectroscopic parameters of the $HOCO^+$ transitions have been retrieved from the JPL database[2] from laboratory measurements by Bogey et al. (1988). Two lines of $HOCO^+$ (the $4_{0,4}$–$3_{0,3}$ and $5_{0,5}$–$4_{0,4}$ at 85.531 and 106.913 GHz, respectively) lie in the frequency range covered by the ASAI survey for upper level energies lower than 30 K and were detected. Their spectra are shown in Fig. 1. Table 1 reports the spectroscopic parameters as well as the properties of the two detected lines, obtained by Gaussian fitting.

For the deuterated form of $HOCO^+$, $DOCO^+$, we used the JPL database with the spectroscopic parameters from Bogey et al. (1986, 1988). Three transitions lie in the frequency range for upper level energies lower than 30 K. In Fig. 2 and Table 1 we present the first tentative detection of this ion using the $5_{0,5}$–$4_{0,4}$ transition, as well as the upper limits on the other transitions. The observed frequency (re-shifted by the 7.2 km s^{-1} V_{LSR} of L1544) is 100 359.81 MHz, compared to the computed 100 359.55 ± 0.035 MHz frequency provided by the JPL database. This is a 0.26 MHz difference and larger than the 0.035 MHz uncertainty quoted for this transition. However, the JPL and CDMS databases do not contain any other transition that could contaminate this frequency, so that we tentatively assign it to $DOCO^+$. New spectroscopic measurements and observations with a lower root-mean square (rms 2 mK for a 10σ detection) are necessary to confirm the detection of the $DOCO^+$ ion.

3. Discussion

3.1. Origin and abundance of $HOCO^+$ and $DOCO^+$

Using the CASSIS[3] software (Vastel et al. 2015b), we first performed a local thermodynamic equilibrium (LTE) analysis of the detected $HOCO^+$ lines of Table 1, where we varied the excitation temperature and $HOCO^+$ column density. The best fit of the two lines is obtained with a column density of 1.9×10^{11} cm^{-2} and an excitation temperature of 8.5 K (see Fig. 1). As a second step, we performed a non-LTE modelling using the LVG code by Ceccarelli et al. (2003) and the collision rates between $HOCO^+$ and

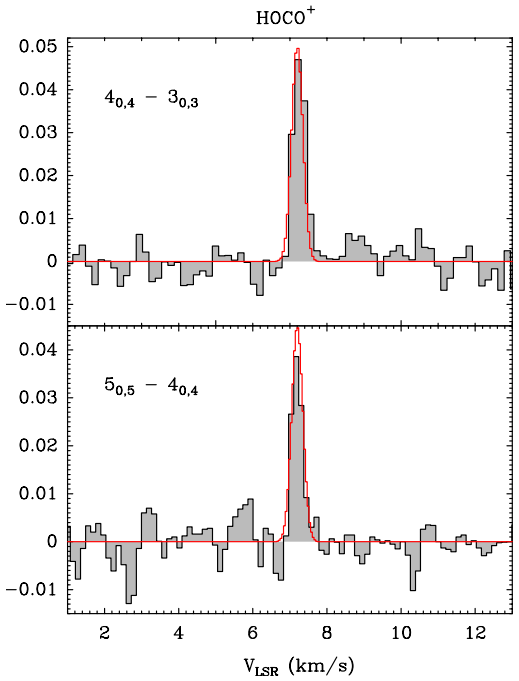

Fig. 1. Detected transitions of $HOCO^+$ (T_{mb}). The red lines correspond to the LTE model (see text).

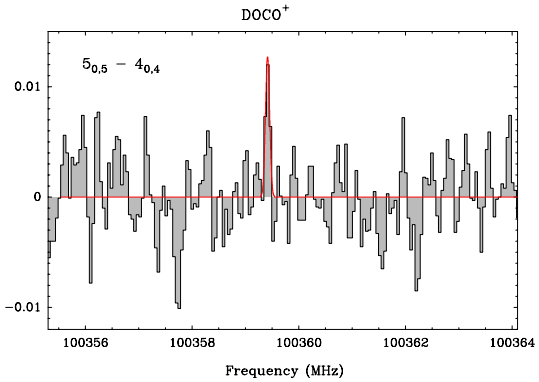

Fig. 2. Tentative detection of $DOCO^+$ (T_{mb}). The red line corresponds to the LTE model (see text). The non-detection if the 80.3 GHz transition is consistent with the derived column density, taking the 5.2 mK rms into account. The modelled 80.3 GHz has the same intensity as the 100.4 GHz transition.

[2] http://spec.jpl.nasa.gov/
[3] http://cassis.irap.omp.eu

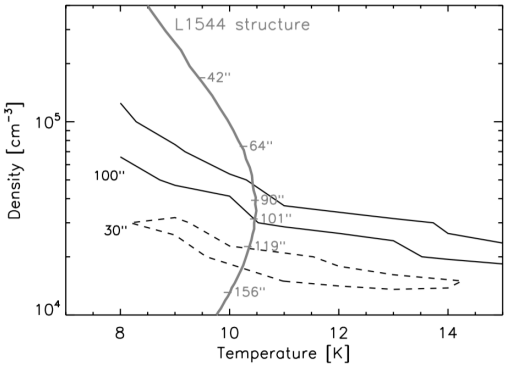

Fig. 3. χ^2 contour plot of the density versus temperature obtained by the non-LTE LVG analysis of the two detected $HOCO^+$ lines for two different source sizes and $HOCO^+$ column densities: 30″ and 6×10^{11} cm^{-2} (dashed line), 100″ and 2.5×10^{11} cm^{-2} (solid line). The thick grey line shows the density-temperature structure of L1544 as derived by Caselli et al. (2012). The ticks along this line show the distance from the L1544 core center, in angular diameter.

helium computed by Hammami et al. (2007), scaled by a factor of 1.37 to take the difference in mass of H_2 into account. The collisional coefficients and spectroscopic data were retrieved from the BASECOL database[4]. The non-LTE LVG analysis shows a degeneracy in the density-temperature space. In order to lift this, we used the same method as in Paper I: we plotted the χ^2 contours superimposed on the density-temperature curve of the physical structure of L1544 as derived by Caselli et al. (2012). The result is shown in Fig. 3. The two sets, LVG analysis and physical structure, cross for a diameter of the $HOCO^+$ emitting region equal to about 100″ (the emission is extended), and a $HOCO^+$ column density of 2.5×10^{11} cm^{-2}. This situation is similar to what has been observed for the methanol emission, which we described in Paper I. For both methanol and $HOCO^+$, the emission originates in the outer layers of L1544 rather than in its dense inner core. The H_2 column density of this outer layer is $\sim 5 \times 10^{21}$ cm^{-2} (see Paper I), which therefore yields a $HOCO^+$ abundance of $(5 \pm 2) \times 10^{-11}$ with respect to H_2.

For $DOCO^+$ we assumed the same excitation temperature as $HOCO^+$, namely 8.5 K, and evaluated its column density to be $\sim 5 \times 10^{10}$ cm^{-2}. Therefore, the upper limit on the $DOCO^+$ abundance is $\sim 10^{-11}$ and the deuteration ratio $DOCO^+/HOCO^+$ is lower than ~25%. We note that the upper limits on the 80.3 and 79.8 GHz $DOCO^+$ transitions are compatible with this estimate.

3.2. Chemical modelling and CO_2 gaseous abundance

The formation of the $HOCO^+$ ion is linked to HCO^+, and we can consider two main formation routes : OH + CO → CO_2 followed by

$$CO_2 + H_3^+ \xrightarrow{k_1} HOCO^+ + H_2 \quad (1)$$

$$CO + H_3^+ \xrightarrow{k_2} HCO^+ + H_2 \text{ followed by}$$

$$HCO^+ + OH \xrightarrow{k_3} HOCO^+ + H. \quad (2)$$

The other relevant formation and destruction rates for $HOCO^+$ and HCO^+ are

$$HOCO^+ + CO \xrightarrow{k_4} HCO^+ + CO_2$$

$$HCO^+ + e^- \xrightarrow{k_5} H + CO$$

$$HCO^+ + H_2O \xrightarrow{k_6} H_3O^+ + CO$$

$$HOCO^+ + e^- \xrightarrow{k_7} H + O + CO$$

$$HOCO^+ + H_2O \xrightarrow{k_8} H_3O^+ + CO_2.$$

At steady state, we can therefore express the $[HOCO^+]/[HCO^+]$ ratio as the following:

$$\frac{[HOCO^+]}{[HCO^+]} = \frac{k_1[H_3^+][CO_2]+k_3[HCO^+][OH]}{k_4[CO]+k_7[e^-]+k_8[H_2O]} \frac{k_5[e^-]+k_6[H_2O]+k_3[OH]}{k_2[CO][H_3^+]+k_4[HOCO+][CO]} \quad (3)$$

$HOCO^+$ was first proposed by Herbst et al. (1977) as an indirect tracer of gas-phase CO_2 and was more recently used for this purpose by Sakai et al. (2008) and Neill et al. (2014). However, they neglected reaction 2 between HCO^+ and OH and obtained a simple relation between $[HOCO^+]/[HCO^+]$ and $[CO_2]/[CO]$ at steady state. The reaction rates (at 10 K) relevant to the formation and destruction of $HOCO^+$ and HCO^+ using the KIDA network[5] are the following (in cm^3 s^{-1}): $k_1 = 1.90 \times 10^{-9}$, $k_2 = 2.47 \times 10^{-9}$, $k_3 = 5.56 \times 10^{-9}$, $k_4 = 1.03 \times 10^{-9}$, $k_5 = 2.93 \times 10^{-6}$, $k_6 = 1.23 \times 10^{-8}$, $k_7 = 7.14 \times 10^{-6}$, and $k_8 = 1.14 \times 10^{-8}$. Both reactions 1 and 2 must be taken into account, and the latter cannot be neglected, leading to an indirect estimate of the $[CO_2]/[CO]$ ratio from $[HOCO^+]/[HCO^+]$. In the centre of the prestellar core region, CO is highly depleted (Caselli et al. 1999) from the gas phase and is unlikely to produce HCO^+ and therefore $HOCO^+$. As a consequence, the $HOCO^+$ ion might be visible in an external layer, where CO is released from the grain surfaces in the gas phase. $HOCO^+$ depends on the cosmic ray ionisation rate ζ_{CR}, which governs the H_3^+ and HCO^+ abundances, and on the CO_2 gaseous abundance when reaction (1) is more efficient than reaction (2). We considered the observations by Vastel et al. (2006), who measured a HCO^+ column density of 4×10^{13} cm^{-2} in the external layer of L1544. If the bulk of the HCO^+ emission arises from the outer layer, whose H_2 column density is 5×10^{21} cm^{-2} (see Sect. 3.1), this yields a HCO^+ abundance equal to $\sim 8 \times 10^{-9}$. Using the measured abundance of both HCO^+ and $HOCO^+$, we can now constrain the gaseous CO_2 abundance. To this end, we ran the Nahoon gas-phase chemical model (Wakelam et al. 2015) and compared the predicted and measured abundance of $HOCO^+$ and HCO^+.

Nahoon computes the chemical evolution of a species as a function of time for a fixed temperature and density. The chemical network kida.uva.2014 contains 6992 unique chemical reactions and in total 7506 rate coefficients, and these reactions involve 489 different species. We built upon the model described in Paper I, that is, we considered a two-step model where in the first step we let the chemical composition reach steady state, and in the second step we injected a variable amount of CO_2 in the gas phase and injected methanol (6×10^{-9} with respect to H atoms) and ethene (5×10^{-9}), as in Paper I, to reproduce the detected COMs described there. The underlying hypothesis is that the gaseous CO_2 is injected by the non-thermal desorption of iced CO_2, as in the case of methanol (Paper I).

For the first step model, we adopted an elemental gaseous carbon abundance of 5×10^{-5} and a C/O ratio equal to 0.5, cosmic ionisation rate ζ_{CR} of 3×10^{-17} s^{-1}, H density of 2×10^4 cm^{-3}, temperature of 10 K and $A_v = 10$ mag, as used in Paper I. The steady abundances of $HOCO^+$ and HCO^+ are 4×10^{-11} and 10^{-8}, respectively; this is fully consistent with the observed ones. We note that a higher C/O ratio of unity will decrease to about 5×10^{-12} for $HOCO^+$ and show no substantial change for HCO^+. We used this two-step model to derive an upper limit to the quantity of injected CO_2, taking the error bars on the observed $HOCO^+$ into account. To stay below the upper value of the $HOCO^+$ abundance (7×10^{-11}), the quantity of injected CO_2 in the gas-phase (through the second step) must be $\leq 2 \times 10^{-6}$

[4] http://basecol.obspm.fr/

[5] http://kida.obs.u-bordeaux1.fr

(with respect to H_2), namely ~4% of gaseous CO. We note that no CO_2 injection in the gas phase is compatible with our $HOCO^+$ observed abundance of 5×10^{-11}, with a abundance (w.r.t. H_2) from the gas-phase chemical modelling of 2×10^{-7}. This value is consistent with the tentative gas-phase abundance average over the line of sight of four deeply embedded massive young stars, (van Dishoeck et al. 1996), the value found in the direction of Orion-IRc2/BN (Boonman et al. 2003a) as well as the average value found towards 8 massive protostars (Boonman et al. 2003b). The inferred abundance is also lower than the solid-state abundances of ~1–3 $\times 10^{-6}$ (Gerakines et al. 1999). Our study leads to the first indirect estimate of the CO_2 presence in the earliest phases of low-mass star-forming regions, with no confusion between hot, warm and cold gas.

Putting together the previous observations in L1544 provides us with a rough estimate of the composition of the grain mantles of a prestellar core, which can only be guessed by the indirect process of non-thermal desorption. It turns out that the mantles should contain methanol, ethene and water, while it is not clear that frozen CO_2 is present. Indeed, to convert the quoted abundances of gaseous into frozen species one has to take into account the relevant efficiency of the non-thermal desorption. Three mechanisms are invoked in the literature: FUV photo-desorption, cosmic-rays and chemical desorption. The latter seems to be very inefficient for the methanol release, based on laboratory experiments (Minissale et al. 2016). Cosmic-rays are suspected to be responsible for the re-injection into the gas phase of CO and other species with low binding energies via hot spot heating ~1000 K (Leger et al. 1985; Shen et al. 2004). However, this mechanism is not efficient in releasing more strongly bonded molecules. Another possibility is that frozen molecules are injected into the gas phase by the FUV photons created by the cosmic-ray interaction with H_2 molecules. Very recent experimental works show for the FUV photo-desorption that methanol has a very low yield, $\leq 10^{-5}$ molecules/photon (Bertin et al. 2016), and that the FUV photons impinging on a methanol ice desorb fragments of the molecule, including CH_3O, with the same efficiency. Our value for the methanol abundance and our upper limit on the CH_3O abundance (respectively 6×10^{-9} and $\leq 1.5 \times 10^{-10}$; Paper I) differ from these experiments, however. In laboratory experiments, CO_2 is desorbed from a pure CO_2 ice FUV illuminated with a yield of $\sim 10^{-4}$ molecules/photon (Martín-Doménech et al. 2015). Assuming the FUV photo-desorption is the dominating mechanism and neglecting the dependence of the photo-desorption yield on the FUV illuminating field, our observations would then indicate a relative composition of the ice as follows: iced-CO_2 ≤20 times iced methanol.

3.3. Deuteration of $HOCO^+$

A high deuterium fractionation has been detected in the L1544 prestellar core where CO is depleted from the gas phase (Caselli et al. 1999). Caselli et al. (2003) detected a strong H_2D^+ emission, and Vastel et al. (2006) found that this ion is extended over the whole core, concluding that H_2D^+ is one of the main molecular ions in the central dense and cold region. Vastel et al. (2006) also detected a correlation between the H_2D^+ abundance and the ratio of DCO^+/HCO^+ and N_2D^+/N_2H^+ as well as the depletion factor, because H_2D^+ is the main driver for deuteration when CO is depleted onto the grain surfaces. L1544 is the site for many first detections in prestellar cores. For example, H_2O has been detected with the *Herschel*/HIFI instrument (Caselli et al. 2012), but deuterated water is unfortunately not detected in this source, although an upper limit on the D/H ratio has been determined from deep observations with the APEX telescope (Quénard et al. 2016). The deuterated form of $HOCO^+$ is likely produced through the high abundance of the H_2D^+ ion that appears extended in the L1544 core (Vastel et al. 2006), coupled with the non-thermal desorption of CO_2 in the external layer. Both H_2D^+ and DCO^+ detected in this core are expected to contribute to the production of the $DOCO^+$, although no deuterated chemical network is available at the moment. The DCO^+/HCO^+ ratio in the external envelope is about 1%, which is much lower than the upper limit of 25% for the $DOCO^+/HOCO^+$ ratio using our tentative detection.

4. Conclusions

We detected two transitions of the $HOCO^+$ ion at 85.5 and 106.9 GHz and obtained a tentative detection of a low energy level transition of its deuterated form at 100.3 GHz. Based on the $HOCO^+$ detections, we were able to estimate the column density and abundance, which was compared to a chemical modelling, constraining the properties and formation of HOCO+ at the early stages towards collapse. The result shows that our detection is compatible with an emission in an external layer, with a CO_2/H_2 abundance of 2×10^{-7} and an upper limit of 2×10^{-6}.

References

Bertin, M., Romanzin, C., Doronin, M., et al. 2016, ApJ, 817, L12
Bogey, M., Demuynck, C., & Destombes, J. L. 1984, A&A, 138, L11
Bogey, M., Demuynck, C., & Destombes, J. L. 1986, J. Chem. Phys., 84, 10
Bogey, M., Demuynck, C., Destombes, J. L., & Krupnov, A. 1988, J. Mol. Struct., 190, 465
Boonman, A. M. S., van Dishoeck, E. F., Lahuis, F., et al. 2003a, A&A, 399, 1047
Boonman, A. M. S., van Dishoeck, E. F., Lahuis, F., Doty, S. 2003b, A&A, 399, 1063
Caselli, P., Walmsley, C. M., Tafalla, M., et al. 1999, ApJ, 523, L165
Caselli P., Walmsley C. M., Zucconi A. et al. 2002, ApJ, 565, 331
Caselli P., van der Tak, F. F. S., Ceccarelli, C., & Bacmann, A. 2003, A&A, 403, L37
Caselli, P., Keto, E., Bergin, E. A., et al. 2012, ApJ, 759, L37
Ceccarelli, C., Maret, S., Tielens, A. G. G. M., et al. 2003, A&A, 410, 587
Gerakines, P. A., Whittet, D. C. B., Ehrenfreund, P., et al. 1999, ApJ, 522, 357
Hammami, K., Lique, F., Jaïdane, N., et al. 2007, A&A, 462, 789
Herbst, E., Green, S., Thaddeus, P., & Klemperer, W. 1977, ApJ, 215, 503
Ioppolo, S., van Boheemen, Y., Cuppen, H. M., et al. 2011, MNRAS, 413, 2281
Jamieson, C. S., Mebel, A. M., & Kaiser, R. I. 2006, ApJS, 163, 184
Leger, A., Jura, M., & Omont, A. 1985, A&A, 144, 147
Martín-Doménech, R., Manzano-Santamaría, J., Muñoz Caro, G. M., et al. 2015, A&A, 584, A14
Minh, Y. C., Irvine, W. M., & Ziurys, L. M. 1988, ApJ, 334, 175
Minh, Y. C., Brewer, M. K., Irvine, W. M. et al. 1991, A&A, 244, 470
Minissale, M, Moudens, A, Baouche, S. et al. 2016, MNRAS, accepted
Neill, J. L., Bergin, E. A., Lis, D. C., et al. 2014, ApJ, 789, 8
Öberg, K. I., Boogert, A. C. A., Pontoppidan, K. M., et al. 2011, ApJ, 740, 109
Podio, L., Lefloch, B., Ceccarelli, C., et al. 2014, A&A, 565, A64
Pontoppidan, K. M., Fraser, H. J., Dartois, E., et al. 2003, A&A, 408, 981
Quénard, D., Taquet, V., Vastel, C., et al. 2016, A&A, 585, A36
Sakai, N., Sakai, T., Aikawa, Y., & Yamamoto, S. 2008, ApJ, 675, L89
Shen, C. J., Greenberg, J. M., Schutte, W. A., van Dishoeck, E. F. 2004, A&A, 415, 203
Thaddeus, P., Guelin, M., & Linke, R. A. 1981, ApJ, 246, L41
Turner, B. E., Terzieva, R., & Herbst, E. 1999, ApJ, 518, 699
van Dishoeck, E. F., Helmich, F. P., de Graauw, T., et al. 1996, A&A, 315, L349
Vastel, C., Caselli, P., Ceccarelli, C., et al. 2006, ApJ, 645, 1198
Vastel, C., Ceccarelli, C., Lefloch, B., & Bachiller, R. 2014, ApJ, 795, L2
Vastel, C., Yamamoto, S., Lefloch, B., Bachiller, R. 2015a, A&A, 582, L3
Vastel, C., Bottinelli, S., Caux, E., et al. 2015b, SF2A-2015: Proc. Annual meeting of the French Society of Astronomy and Astrophysics, 313
Wakelam, V., Loison, J.-C., Herbst, E., et al. 2015, ApJS, 217, 20
Watanabe, N., & Kouchi, A. 2002, ApJ, 567, 651
Whittet, D. C. B., Gerakines, P. A., Tielens, A. G. G. M., et al. 1998, ApJ, 498, L159
Whittet, D. C. B., Shenoy, S. S., Bergin, E. A, et al. 2007, ApJ, 655, 332
Whittet, D. C. B., Cook, A. M., Chiar, J. E., et al. 2009, ApJ, 695, 94